Design and analysis of a high NA projection optical system for 0.35μm deep-UV lithography

Andrew V. Hill, James E. Webb, Anthony R. Phillips, and James E. Connors

GCA/Tropel, 60 O'Connor Road, Fairport, NY 14450

ABSTRACT

To meet the exacting demands of sub-half micron lithography, rigorous analysis must be a part of the entire optical design process. Several new modeling techniques have been developed to aid in determining the lithographic performance of an optical design. An aerial image modeling program has been implemented for the examination of CD variation and isolated/grouped line bias. Additional models have been developed to examine lens heating effects, stray light, and ghost images. A tolerancing technique has been established which provides maximum manufacturability while allowing minimal performance degradation. This design, analysis, and tolerancing process has yielded the first 31mm field, 0.53 NA, 248nm lithographic objective capable of producing 0.35μm features in a manufacturing environment. The objective, as built, has a maximum astigmatism of 0.20μm and a total focal plane deviation of 0.17μm. A 1.3μm common focus corridor in 1.0μm thick APEX-E has been demonstrated for 0.35μm features over the entire field. A grouped/isolated CD bias of 9nm has been measured. This paper presents the design and analysis procedures along with the experimental results for this objective.

1. INTRODUCTION

The semiconductor industry continues on its incessant quest for finer resolution and larger field sizes from microlithography systems. In order to achieve increased resolution, lithographers are pushing for shorter wavelengths and higher NA's. To maintain the depth of focus required for a robust semiconductor manufacturing process while simultaneously increasing field sizes, lens manufacturers must come much closer to producing a perfect lens than they have in the past. This requires more sophisticated designs, tighter control of the manufacturing processes, and increased stability in the completed systems.

The slim manufacturing margin for a deep-UV objective requires that the impact on lithographic performance of each step of the design and analysis process be scrutinized. Performance is measured during the optical design process using models developed to predict depth of focus, CD variation, and image placement errors. Mechanical design impacts on optical performance are determined by examining stray light and structural integrity. The optical properties of the raw fused silica used to produce finished elements are modeled extensively. And a rigorous technique for tolerancing all aspects of the optical system is employed to optimize manufacturability of the completed design.

2. DESIGN PROCESS

Microlithographic objectives are difficult lenses to design in terms of both performance and manufacturability. Although the design process for lithographic objectives is similar in many ways to that of other lenses, several factors make the process more demanding; specifications are placed on all aspects of optical performance, the designer must deal with a large number of variables, and the designer must locate an acceptable solution in a limitless solution space.

Resolution	0.35μm Lines and Spaces
Depth of Focus	1.2μm Common Corridor
Field Size	31mm Diameter
Image Placement	40nm Max Vector
Field Flatness	±0.125μm
CD Variation	±35nm

Table 1. Lithographic specifications for 3153KrF objective.

0-8194-1161-2/93/$6.00

Downloaded from SPIE Digital Library on 06 Jan 2012 to 199.197.130.217. Terms of Use: http://spiedl.org/terms

The designer is tasked with a list of performance specifications which his design must achieve. *Table 1* gives examples of some of the critical specifications for the 3153KrF "Thistle" program. Only first order parameters are at the designer's disposal for meeting these performance specifications. These parameters are radius of curvature, thickness, glass type, number of elements, spacings between elements, and stop location. Since fused silica is the only viable material for deep-UV objectives, choice of glass is not an available variable at 248nm.

The designer must also meet manufacturing, mechanical, and additional performance constraints beyond the basic specifications. An example of a manufacturing constraint is maximum element thickness; currently limited by the availability of high quality fused silica in large thicknesses. Mask to wafer distance and object and image working distances are examples of fundamental mechanical constraints placed on the optical design. Some additional performance constraints are shown in *Table 2*.

• NA	• Bandwidth	• Color Correction	• Object Angle
• Partial Coherence	• Astigmatism	• Strehl Ratio	• Lens Heating
• Reduction Ratio	• Coma	• RMS Wavefront	• Transmission
• Wavelength	• Spherical Aberration	• Telecentricity	• Temperature Sensitivity

Table 2. Performance and design constraints.

Once the performance specifications and design constraints have been determined, the task of actually designing the system begins. Typically a previous design is used as a starting point for further optimization. Several design paths are taken and as the process proceeds, paths are eliminated and only the most promising are followed. Optimizing routines such as damped least squares, orthonormal optimization, and simulated annealing are used to alter the first order variables until all constraints are met and the best possible performance is achieved. Upon completion of the optimization phase, each potential solution is rigorously analyzed and toleranced before selection of the final design form. The final form is then wrung through a further process of refinement and analysis.

3. DESIGN ANALYSIS

Several different models have been developed for determining the strengths and weaknesses of a lithographic design. All of these models are used to provide the optical designers with instant feedback into the progress of a design. Image contrast through focus provides information on depth of focus and astigmatism. Wavefront analysis is used to gain insight into the nature and balance of higher order aberrations. Aerial image modeling reveals the impact of aberrations on CD sizes throughout the field. And image placement modeling gives an accurate representation of lens distortion.

3.1 Contrast Modeling

Contrast modeling provides valuable information about the changes in an image through focus and at different points in the field. The contrast in an image is generally defined by the equation:

$$contrast = \frac{I_{max} - I_{min}}{I_{max} + I_{min}}$$

where I_{max} is the peak intensity in the image, and I_{min} is the minimum intensity in the image of a grouped line pattern. Contrast can be obtained from any one of many commercially available programs which yield image intensity distributions from either ray tracing through the optical design or from diffraction analysis based on the exit pupil wavefronts of the design .

Figure 1 illustrates how image contrast data can be related to lithographic performance. Data for 0.35μm grouped lines at five different points in the image field is presented. The bottom set of curves is from the center of the image field. The top set is from a corner of the field. At each point in the field, contrast is plotted as a function of focus for both sagittal

Downloaded from SPIE Digital Library on 06 Jan 2012 to 199.197.130.217. Terms of Use: http://spiedl.org/terms

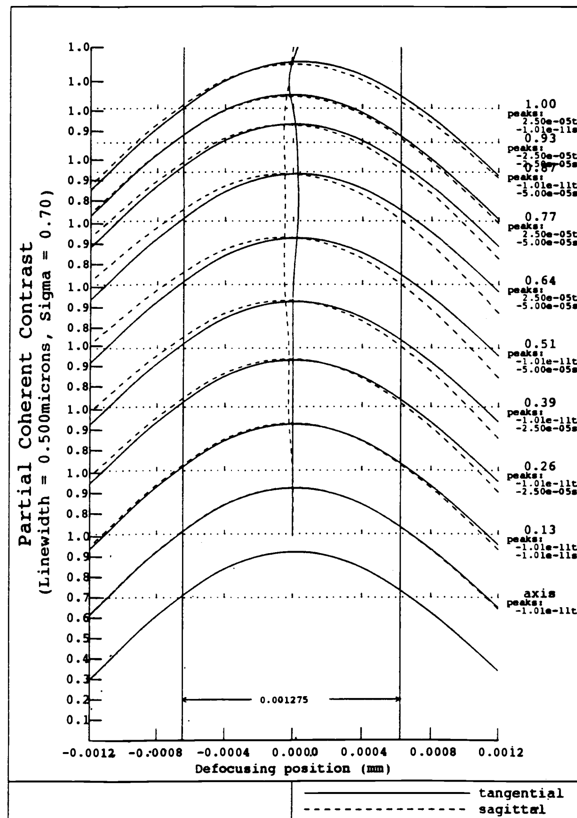

Figure 1. Contrast through focus.

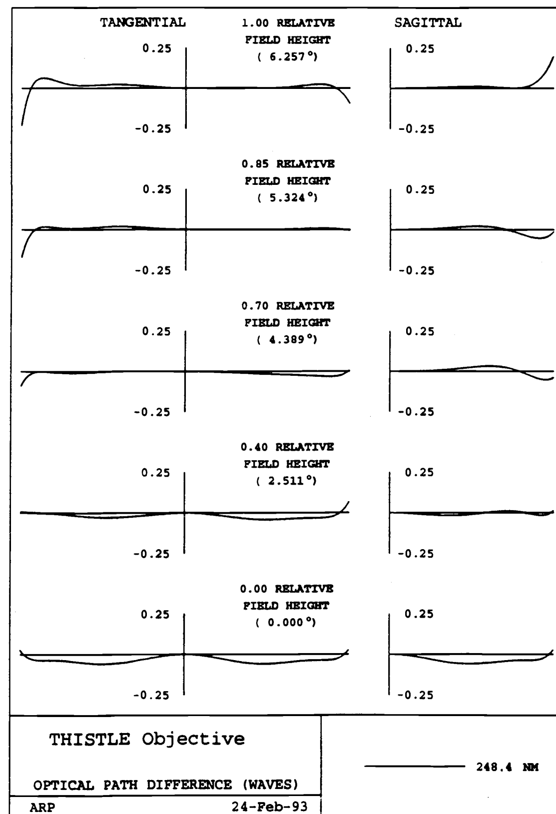

Figure 2. Image wavefront deviations.

and tangential features. The optical designer can use a plot such as this to examine the field curvature and astigmatism of his design. If the contrast level at which a resist can resolve the features is known, depth of focus can also be predicted. Suppression of a contrast curve can also indicate the presence of other aberrations such as coma, spherical aberration and chromatic aberration.

3.2 Wavefront Analysis

Wavefront analysis is part of nearly every optical design and is nothing new to the design of objectives for lithography. However, the performance requirements and complexity of a lithographic objective place more emphasis on higher order aberrations than is typically found in simpler lenses. Wavefront plots are used to obtain a graphical view of the presence and interactions of the low and high order aberrations. This can aid the designer in removing and balancing the residual aberrations.

Figure 2 shows typical wavefront slices for a lithographic objective. The wavefront at the center of the field is shown in the bottom plots and the wavefront at the edge of the field is shown at the top. Units are in wavelengths. Note that there are multiple inflections in each curve, indicating the presence of high order aberrations.

3.3 CD Modeling

CD modeling is relatively new to optical design. Several programs have become commercially available which simulate the effect of wavefront aberrations on the aerial image of complex features. This type of analysis is particularly useful for examining linewidth variations through focus and throughout the field[1]. *Figure 3* shows the variation in aerial image linewidth over a 1.6μm focus range for grouped 0.35μm lines at 7 points in the field. Any variation among the curves is due to aberrations in the wavefront. *Figure 4* shows the difference between grouped and isolated 0.35μm lines over the

Downloaded from SPIE Digital Library on 06 Jan 2012 to 199.197.130.217. Terms of Use: http://spiedl.org/terms

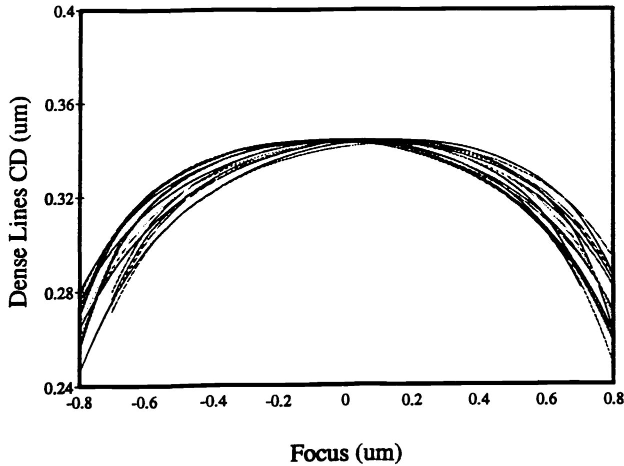

Figure 3. Grouped line CD's through focus.

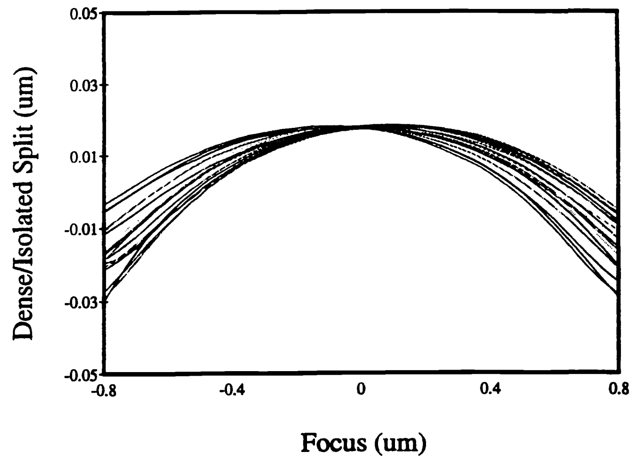

Figure 4. Grouped/Isolated CD bias.

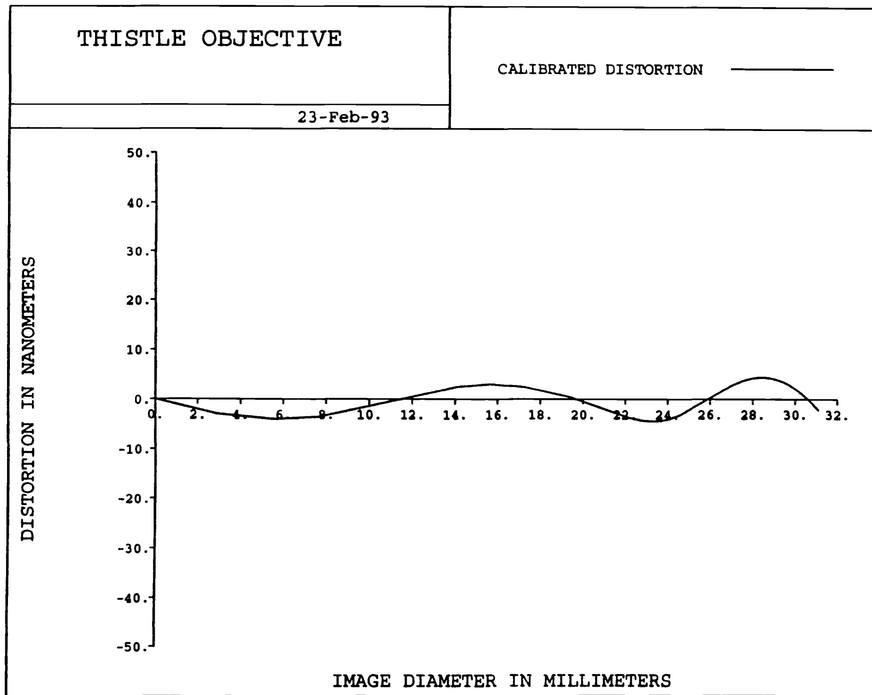

Figure 5. Design distortion for Thistle lens.

same focus range. The separation of the grouped and isolated lines indicates a mean linewidth bias between the two types of features. Both sets of curves give an indication as to the impact of residual aberrations on lithographic performance.

3.4 Image Placement

In very few lens systems is image distortion as critical as in microlithography. Since the distortion in a lithographic objective is measured in nanometers, the common technique of using the chief ray to define image placement is not sufficient. The centroid of a ray bundle gives a more accurate prediction of the actual lens distortion. *Figure 5* is the distortion curve for the Thistle lens design. Deviation from the ideal image location is plotted against distance from the center of the field in nanometers. Since the optical design is radially symmetric, only radial distortion is shown. The maximum vector in the Thistle design can be seen to be 4nm.

Downloaded from SPIE Digital Library on 06 Jan 2012 to 199.197.130.217. Terms of Use: http://spiedl.org/terms

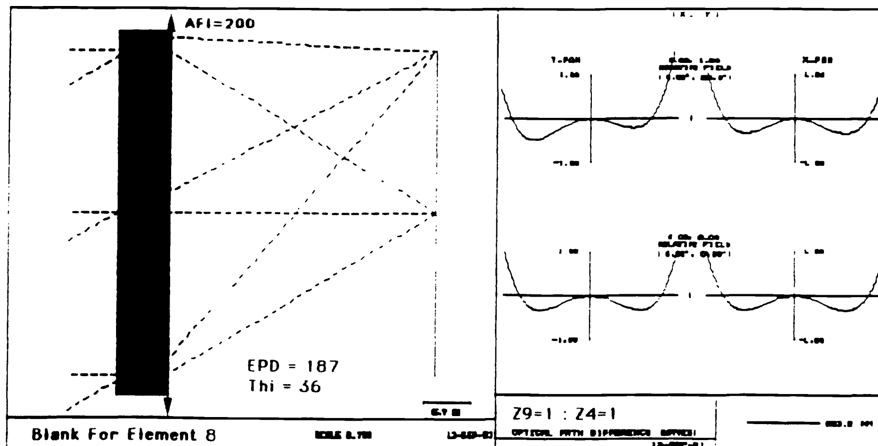

Figure 6. Wavefront transmitted through an inhomogeneous blank.

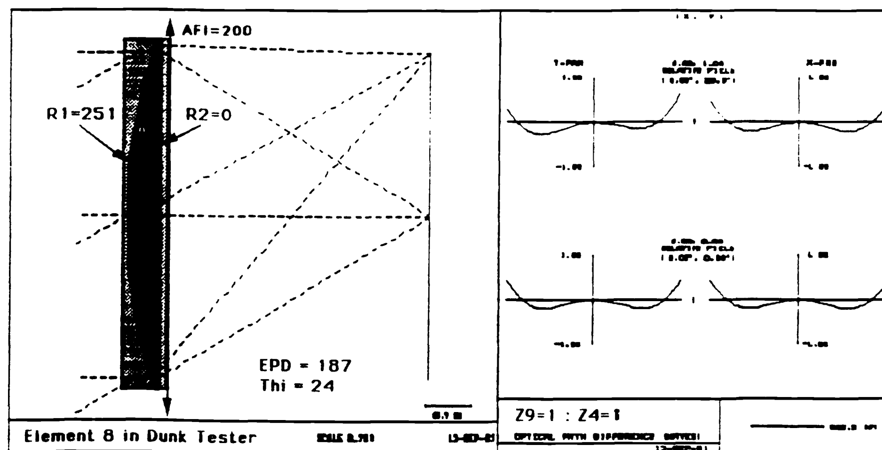

Figure 7. Wavefront transmitted through an inhomogeneous element.

4. CRITICAL DEEP-UV ISSUES

Development of microlithographic objectives for the deep-UV has encountered a number of new issues. Several of these are related to the lack of suitable optical materials other than fused silica. The refinement of line narrowed excimer lasers has minimized the significant issue of color correction, but issues still remain which push the quality of fused silica to new limits. Inhomogeneities in the bulk fused silica create excessive wavefront deviations if they are not closely controlled, and material absorption creates lens heating which has been an issue at i-line and continues to be relevant at deep-UV.

4.1 Material Homogeneity

The process used to produce fused silica is more prone to inhomogeneities than the processes used in the production of other optical glasses. This creates a significant issue for deep-UV objectives which are made solely of fused silica. Inhomogeneities can cause serious degradations in performance similar to the effect of element surface irregularities. Both cause deformations in the transmitted wavefronts which frequently manifest themselves as asymmetries around the image field. The homogeneity requirements for the fused silica used in microlithography are pushing the capabilities of its manufacturers.

Downloaded from SPIE Digital Library on 06 Jan 2012 to 199.197.130.217. Terms of Use: http://spiedl.org/terms

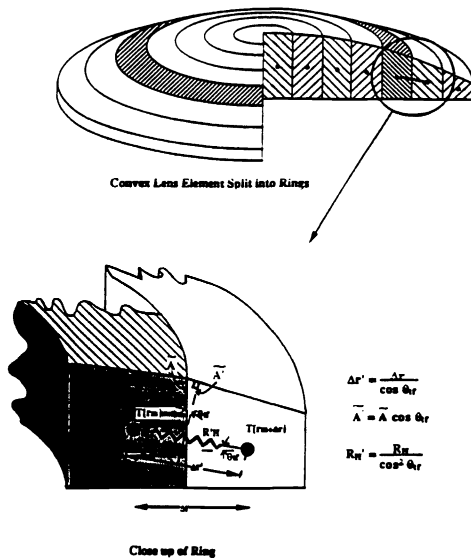

Figure 8. Finite element analysis of radiation absorption.

With specifications at the limits of what can currently be produced, thorough modeling techniques must be employed to ensure that specifications are rigorous. A technique has been developed for modeling the optical impacts of inhomogeneities of any arbitrary shape. *Figure 6* shows an inhomogeneous blank of fused silica with two planar wavefronts passing through it. Wavefront plots show the wavefront deviations created by the inhomogeneities. *Figure 7* shows the same blank, this time shaped into an element and surrounded by homogeneous material. As would be expected, the wavefronts are deviated less at the element's edges where more inhomogeneous material has been removed. With this capability the inhomogeneity of each element in the objective can be measured and its impact on performance can be modeled precisely. This has led to rigorous specifications on fused silica inhomogeneity using the tolerancing techniques described below in section 5.

4.2 Material Absorption

Lens heating has been a common phenomenon in i-line objectives causing drifts in both focus and magnification. The same phenomenon can be encountered in the deep-UV. In both cases heating is caused by absorption of radiation in the optical elements. This absorption can result in index gradients and surface deformations, each of which affect focus and magnification. In i-line lenses the problem can be corrected by appropriate selection of glasses so that the index gradients and surface deformations compensate one another to offset any imaging instabilities. At deep-UV, where fused silica must be used, only the absorption of the material can be minimized to reduce lens heating instabilities.

A thermal model has been developed for the design of i-line objectives which simulates both index gradients and surface deformations due to material absorption. The same model has been used to determine absorption specifications for fused silica. The model uses finite element techniques to simulate absorption, conduction, and convection in all elements of the objective. *Figure 8* illustrates how a slice of an element is broken down into rings. Rings can be used due to the circular symmetry of the objective. Modeling and actual measurements of lens heating have been performed on the Thistle objective and indicate no perceptible shifts in focus or magnification from 1 hour of continuous exposure.

4.3 Stray Light

Stray light or flare in the image plane can result in a loss of exposure latitude. The opto-mechanical design of a lithographic objective must be optimized early in the development process in order to maximize the suppression of stray light. *Figure 9* illustrates an optical model of several elements in an objective. The inner surfaces of the surrounding mechanics are modeled as reflecting surfaces. A stray bundle of light is shown reflecting off a metal surface and making its way to the image plane. Minor modifications of the slope of the offending metal surface can deflect the light sufficiently to prevent external transmission (*Figure 10*). All possible angles of stray light bundles must be examined and appropriate modifications made to ensure that undesired radiation is not transmitted onto the image plane.

Ghost images are another form of stray light which can cause image degradation. A ghost image can be formed by unwanted reflections off element surfaces. These are typically modeled by examining all possible two reflection combinations in a system. In an objective with 20 elements (40 surfaces) there are 761 possible two reflection ghosts. Occasionally a combination will be of sufficient intensity to warrant modification of the optical design. In most cases a

Downloaded from SPIE Digital Library on 06 Jan 2012 to 199.197.130.217. Terms of Use: http://spiedl.org/terms

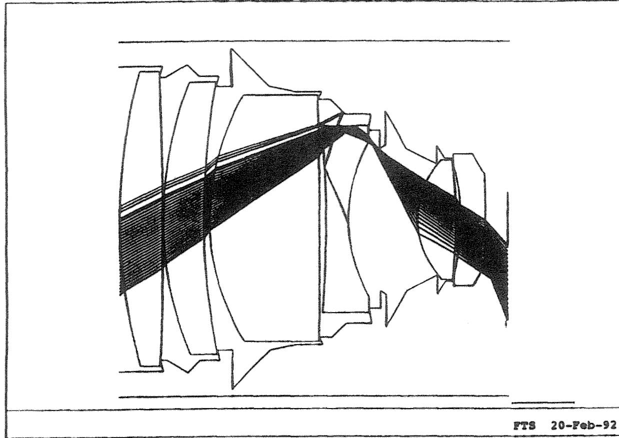

Figure 9. Stray light analysis.

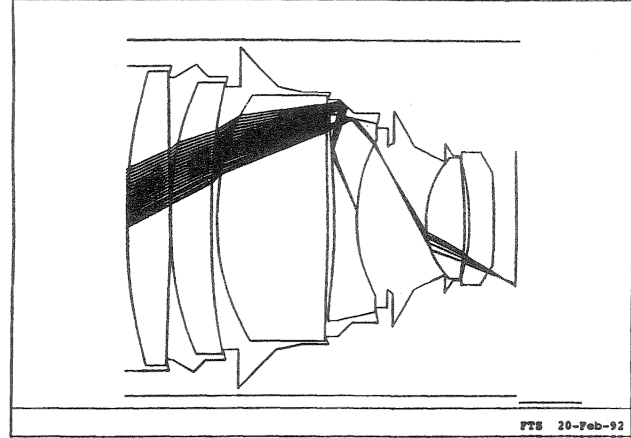

Figure 10. Stray light after modifications.

few surfaces will be identified which will require higher quality anti-reflection coatings and more rigorous reflectance testing.

5. TOLERANCING FOR MANUFACTURING

Rigorous tolerancing of all lens parameters is required in order to produce microlithographic objectives which can meet the necessary performance requirements in a cost effective manner. With the raw fused silica for individual elements costing more than $10,000 and a completed element costing more than $20,000, minimizing scrap and rework in a system with over 20 elements is a great concern. Each element has over 24 major parameters which can cause image degradation and system failure. The assembly process contributes more than 70 additional potential detractors. With so many potential contributors to image degradation, identifying causes of problems once the lens has been assembled can be costly and time consuming. Tolerancing of all lens parameters from raw material purity to final element spacing adjustments must be performed in order to minimize scrap and rework and eliminate causes of image degradation early in the manufacturing process.

Toleranced lens parameters can be placed into three categories; raw material parameters, element fabrication parameters, and lens assembly parameters. Raw material includes refractive index, dispersion, homogeneity, transmission, and blemishes. Element fabrication includes two basic first order parameters; radius and thickness; and higher order parameters such as surface figure and wedge. The remaining parameters are components of lens assembly: element spacings, tilts, and decenters. These three categories account for all of the major optical parameters, and can typically be dealt with on an independent basis.

Lenses have been traditionally toleranced using criteria such as RMS wavefront error, MTF, and chief ray distortion[2]. These criteria are not sufficient for describing lithographic performance during the design process, and the same holds true for the tolerancing process. Criteria such as depth of focus, astigmatism, field flatness, CD control, and centroid distortion must be used in order to determine the impacts of a particular tolerance. These performance measures can be accurately modeled using similar software to that used in the lens design process.

Monte Carlo analysis is a common method of simulating a system with many varying parameters such as a manufacturing process. The statistical distributions for each parameter in the process must be known or approximated. A generating function is derived which can recreate the parameters distribution from a set of random numbers. For example, a parameter may have a normal distribution during manufacturing. The generating function,

$$x_1 = \langle m \rangle + \sigma(-2\ln y_1)^{1/2} \sin 2\pi y_2$$

Downloaded from SPIE Digital Library on 06 Jan 2012 to 199.197.130.217. Terms of Use: http://spiedl.org/terms

produces a normal distribution with mean $\langle m \rangle$ and variance σ when y_1 and y_2 are random numbers from 0 to 1 [3]. If a system is simulated in which each parameter has been allowed to change based on its generating function, the system will closely represent one which may actually be observed. By generating many such systems, accurate predictions can be made as to the expected nature of these systems.

Monte Carlo analysis can be readily applied to modeling the manufacture of a lens system. In the case of a microlithographic objective the varying parameters are those discussed above; radii, thicknesses, etc. The performance measures for the system are also discussed above; depth of focus, distortion, etc. The manufacturing history of each parameter can be compiled to determine its statistical distribution as a function of its tolerance. *Figure 11* illustrates a typical production distribution for thickness as a percentage of tolerance. A similar distribution can be derived for every parameter to be toleranced. Assuming that new tolerances will not significantly alter these distributions, a generating function can be derived which will simulate a parameters distribution based on its new tolerance.

Once the generating functions are known for each parameter, the impact of a given set of tolerances on system performance can be determined. Starting tolerances for every parameter in the system may be selected initially based on past experience. Applying these tolerances, each parameter is varied from its nominal value by a random amount determined by its generating function. With all parameters in a perturbed state, the system represents a lens which might be manufactured under these set of tolerances. By generating many such perturbed systems, statistics can be calculated on the simulated systems to determine the average and variance of each modeled performance criterion. *Figure 12* shows the distortion measured in 50 such simulated systems. A running average and standard deviation is also plotted. Stabilization of the running mean and standard deviation indicates that sufficient systems have been simulated to evaluate the results. This method gives an accurate picture as to the impact of a chosen set of tolerances on system performance. However, if the impact is unacceptable, it gives very little insight into how the tolerances should be adjusted. With several hundred parameters varying simultaneously, it is difficult to determine which tolerances are the significant contributors to performance degradation.

A sensitivity analysis can be used to assist in determining the relative significance of contributors. To determine the relative sensitivities of each of the parameters, a nominal system is modeled with one parameter perturbed by a small amount. The impact of this perturbation is then determined on the system. This is done successively for each parameter and each evaluation criterion. A sample result is shown in *Figure 13* for the sensitivity of distortion to element thickness deviations. The most sensitive thickness has been normalized to 1. A curve such as this can be linked directly to tolerances by a scaling factor.

Using this technique, relative tolerances for sets of parameters are determined by a sensitivity analysis. Scaling factors for each set of parameters determine their actual tolerances. Finally, Monte Carlo analysis is used to evaluate the impacts of the scaling factors for a given set of tolerances. In this way a system of hundreds of critical parameters can be rigorously toleranced by adjusting only a few scaling factors.

6. PERFORMANCE RESULTS

A prototype 3153KrF "Thistle" objective has been built using the design, analysis, and tolerance processes described above. The objectives performance has been compared against the initial specifications supplied to the designers. Resolution, depth of focus, CD control, and image placement errors have all been measured and analyzed.

6.1 Resolution

Resolution and depth of focus define the minimum critical dimension for a given lens and the process latitude for each feature size. A feature can be considered resolved if it meets several criteria. The feature must fall within a CD limit, the resist must not scum between features, the resist sidewalls must exceed a certain limit, and there may be no loss of resist on the top of the feature. For the resolution data presented here, no CD's are outside ±10% of nominal, and all sidewalls are greater than 85°. All depth of focus numbers reported here represent a common "usable" depth over the entire field. 21 points in the field are measured to determine the common depth of focus. 3 die are measured in a SEM with each field point being averaged to reduce wafer flatness effects. Tips are removed from the data to isolate stepper and wafer effects

Downloaded from SPIE Digital Library on 06 Jan 2012 to 199.197.130.217. Terms of Use: http://spiedl.org/terms

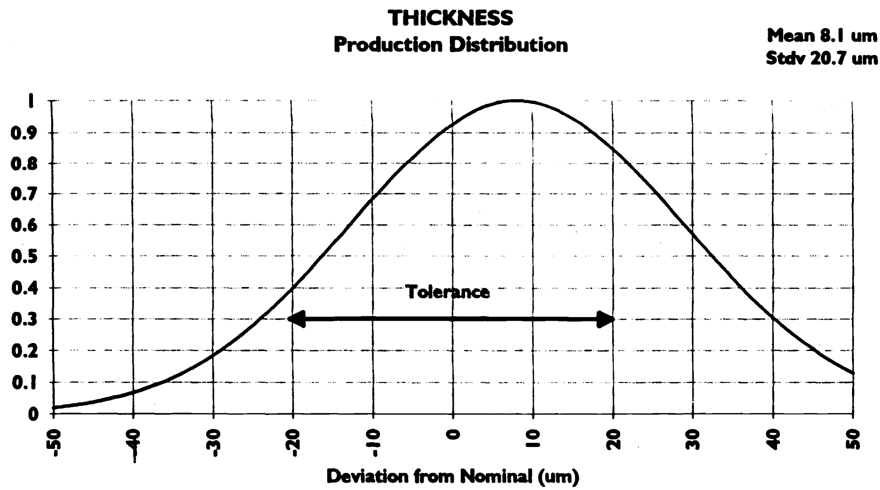

Figure 11. Manufacturing distributions for element thickness.

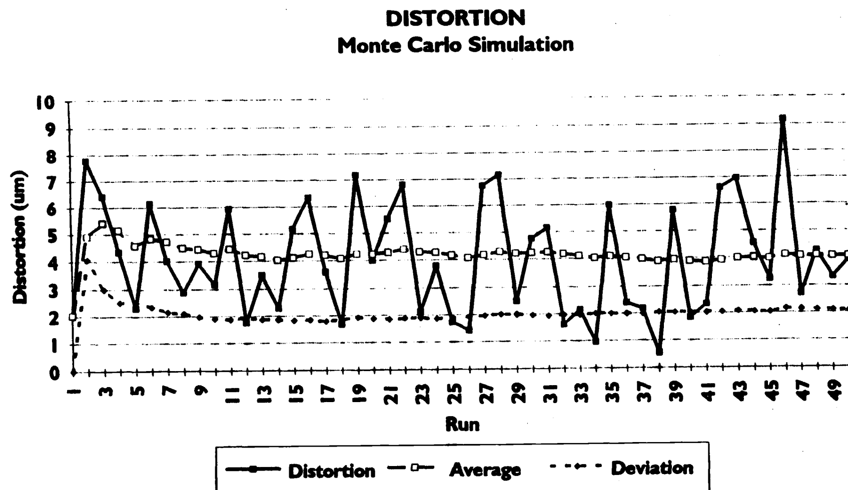

Figure 12. Monte Carlo simulation of lens distortion.

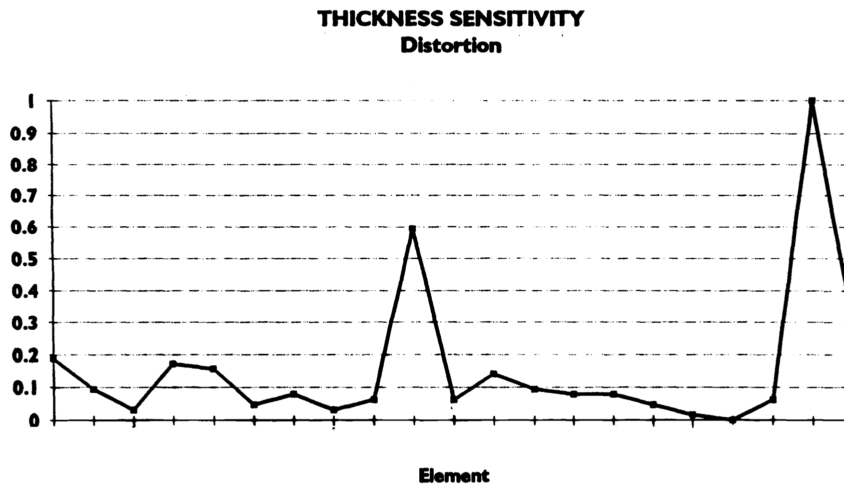

Figure 13. Sensitivity of distortion to element thickness.

Downloaded from SPIE Digital Library on 06 Jan 2012 to 199.197.130.217. Terms of Use: http://spiedl.org/terms

from actual lens performance. *Table 3* summarizes the depth of focus results for various feature types and resists. At an NA of 0.53, 0.17μm of astigmatism and 0.20μm (±0.10μm) of field flatness were measured. Actual SEM photographs of 0.35μm lines in 1μm of APEX-E resist are shown over a 1.6μm depth of focus in *Figure 14*.

Feature Size	Feature Type	Resist	NA	σ	DOF
0.35μm	Isolated & Grouped	1μm APEX-E	0.53	0.74	1.3μm
0.35μm	Contacts	1μm APEX-E	0.53	0.74	1.0μm
0.40μm	Isolated & Grouped	1μm APEX-E	0.42	0.73	2.0μm
0.40μm	Contacts	1μm APEX-E	0.42	0.73	1.3μm
0.25μm	Isolated & Grouped	0.6μm XP89-131	0.53	0.74	0.7μm
0.25μm	Grouped	1μm APEX-E	0.53	0.74 Annular	1.3μm

Table 3. Common corridor depth of focus for 3153Krf Thistle lens.

6.2 CD Control

Two linewidth measurements are of particular importance; variations of CD and the difference in mean CD's for isolated and grouped lines. *Figure 15* is a frequency histogram of 0.35μm dense feature CD's for horizontal and vertical orientations at 21 points in the field and at best focus and the two extremes of defocus for a total of 126 data points. The mean is calculated at 0.343μm with a 3σ of 31nm. Measurements of 0.35μm isolated features are shown in *Figure 16*. The mean for isolated features is 0.352μm with a 3σ of 40nm. Note the 9nm difference between dense line and isolated line means. Both dense and isolated results are combined in the histogram in *Figure 17*. The mean here is 0.347μm with a 3σ of 38nm. All of these measurements are within the specification of 0.35μm ± 10% for CD variation.

6.3 Image Placement

Image placement errors are a critical component in total overlay budgets. These errors were measured on the Thistle lens using the insitu metrology system in the stepper. This system scans a slit over the image of a line at a specified number of points in the field. Distance measuring interferometers on the stages are used to compare the measured location of each image to a perfect grid. By averaging 20 such sets of measurements, an accurate representation of image placement errors can be obtained.

A mapping of placement errors for the Thistle lens is shown in *Figure 18* at 601 points in the field. The circles represent the nominal image locations and the lines represent vectors to the measured images. Histogram summaries of this data are shown in *Figure 19* for errors in both the X and Y directions. The X direction measurements show a maximum vector of 38 nm and a 3 sigma of 39 nm. The Y direction measurements are slightly better with a maximum vector of 33 nm and a 3 sigma of 33 nm. By definition the mean in both the X and Y directions is zero. A radial average of the image placement errors is shown in *Figure 20*. The magnitude of these measurements compares well with the radial distortion curve predicted from the optical design (*Figure 5*).

7. SUMMARY

A 3153KrF objective has been designed and thoroughly analyzed to ensure manufacturability and conformance to specification. Several analytical models including a tolerancing technique have been developed which critique performance in terms critical to microlithography. The critical deep-UV issue of fused silica quality has been addressed rigorously by an inhomogeneity model and an absorption model.

A prototype objective was built to tolerance and found to exceed all specifications. A 1.3μm common corridor depth of focus was measured for 0.35μm grouped and isolated features over a 31mm diameter field. The maximum astigmatism measured 0.17μm and field flatness, 0.20μm. All linewidths fell within the ±10% window, with a mean difference between grouped and isolated lines of less than 10nm. 601 image placement measurements found a maximum distortion vector of 39nm. No lens heating or stray light was detectable.

Downloaded from SPIE Digital Library on 06 Jan 2012 to 199.197.130.217. Terms of Use: http://spiedl.org/terms

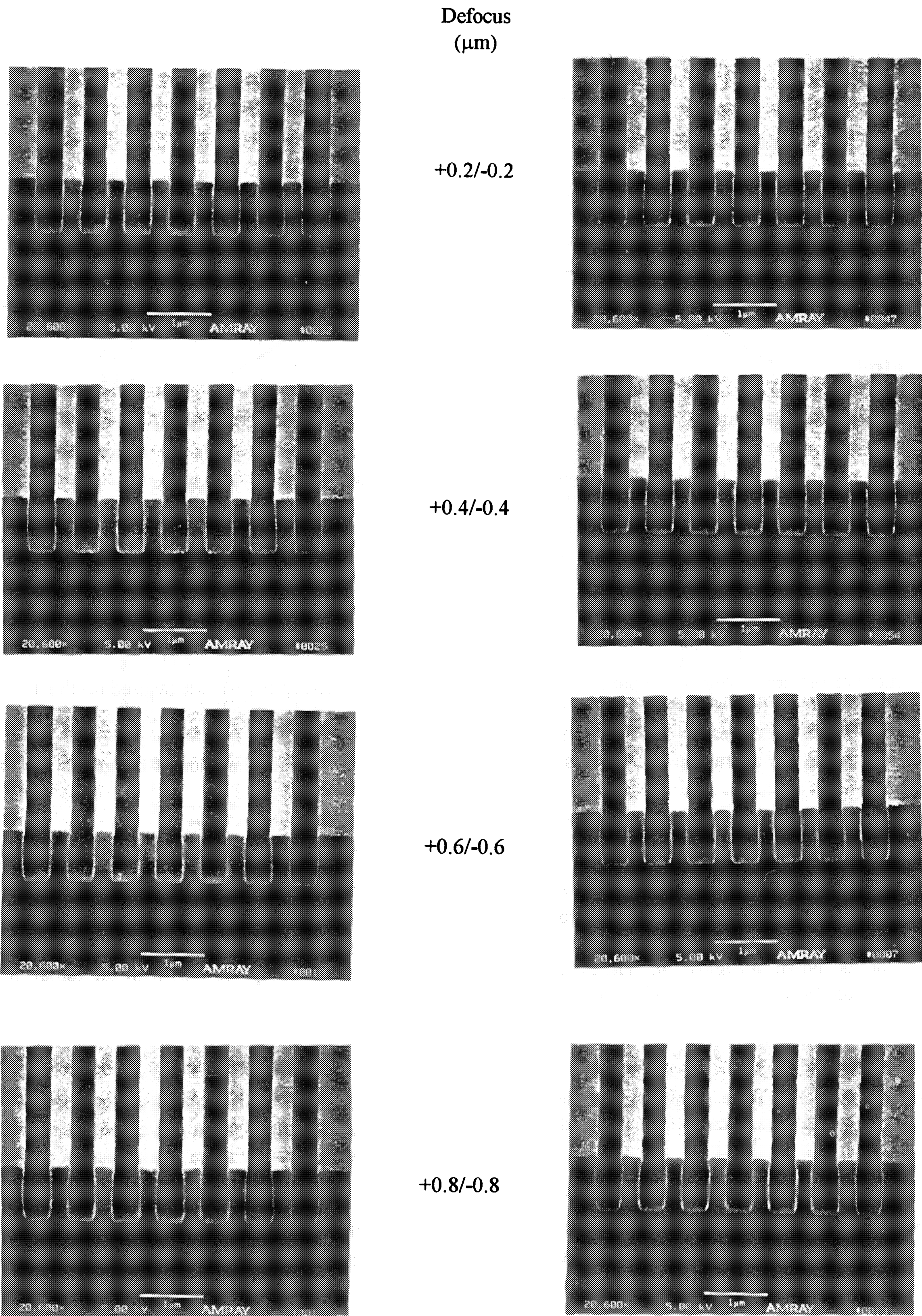

Figure 14. 0.35μm lines and spaces through focus.

Downloaded from SPIE Digital Library on 06 Jan 2012 to 199.197.130.217. Terms of Use: http://spiedl.org/terms

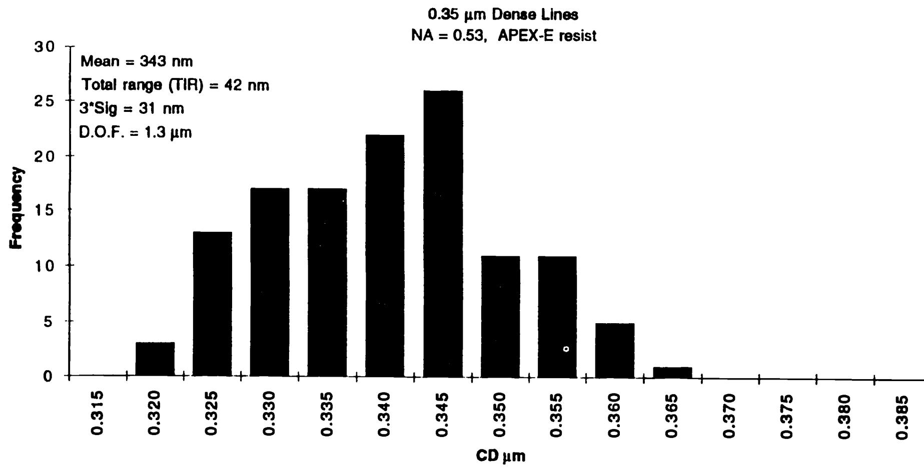

Figure 15. CD measurements of 0.35μm grouped lines.

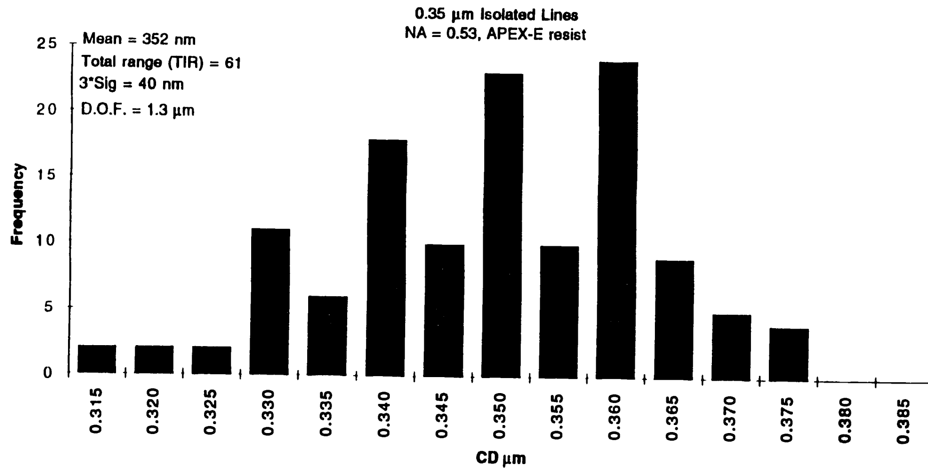

Figure 16. CD measurements of 0.35μm isolated lines.

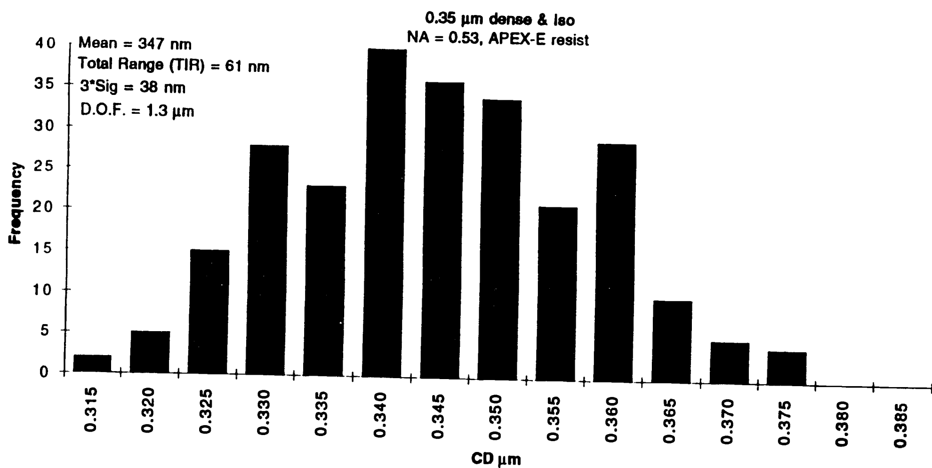

Figure 17. CD measurements of 0.35μm grouped and isolated lines combined.

Downloaded from SPIE Digital Library on 06 Jan 2012 to 199.197.130.217. Terms of Use: http://spiedl.org/terms

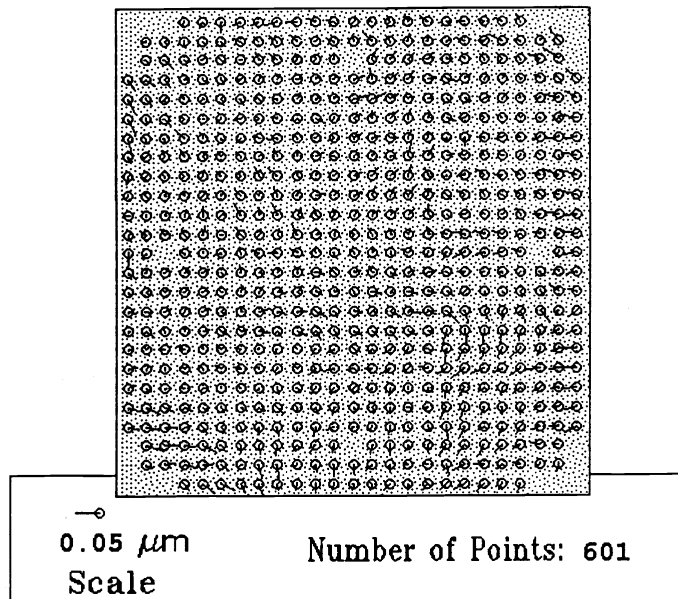

Figure 18. Distortion vector map.

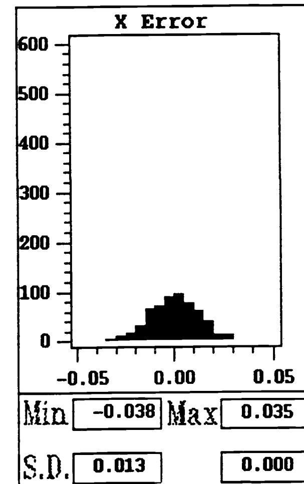

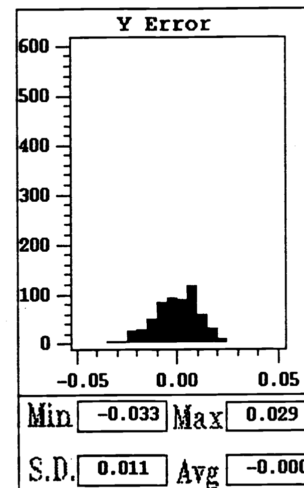

Figure 19. Distortion histograms.

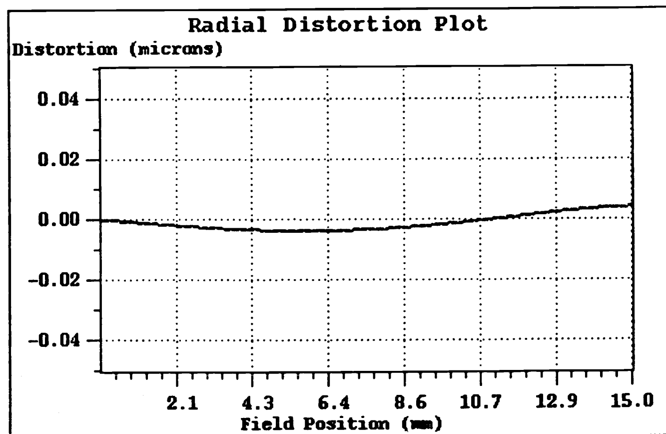

Figure 20. Radial Distortion.

8. ACKNOWLEDGMENTS

The authors would like to thank SEMATECH and its member companies for their support of the Thistle development program and for their technical input throughout this design process. Also to be thanked are J. Bruning, D. Beaulieu, and G. Kahwati for their leadership of the Thistle program and especially the dozens of Tropel emloyees whose efforts brought about its success.

9. REFERENCES

1. J.E. Connors, et. al., "Advanced lithography simulation tools for development of high numerical aperture projection optical systems," *SPIE Symposium on Microlithography Proceedings*, March 1993.
2. M.P. Rimmer, "A tolerancing procedure based on modulation transfer function (MTF)," *SPIE Vol. 147 Computer Aided Optical Design*, pp. 66-68, 1978.
3. B.R. Frieden, *Probability, Statistical Optics, and Data Testing*, Springer-Verlag, New York, 1983.

Downloaded from SPIE Digital Library on 06 Jan 2012 to 199.197.130.217. Terms of Use: http://spiedl.org/terms